

MeLPUF: Memory in Logic PUF

Christopher Vega, Patanjali SLPSK, Shubhra Deb Paul, Swarup Bhunia
{c.vega,patanjali.sristil,shubhra.paul}@ufl.edu,swarup@ece.ufl.edu
University of Florida

ABSTRACT

Physical Unclonable Functions (PUFs) are used for securing electronic designs across the implementation spectrum ranging from lightweight FPGA to server-class ASIC designs. However, current PUF implementations are vulnerable to model-building attacks; they often incur significant design overheads and are challenging to configure based on application-specific requirements. These factors limit their application, primarily in the case of the system on chip (SoC) designs used in diverse applications. In this work, we propose MeL-PUF– Memory-in-Logic PUF, a low-overhead, distributed, and synthesizable PUF that takes advantage of existing logic gates in a design and transforms them to create cross-coupled inverters (i.e. memory cells) controlled by a PUF control signal. The power-up states of these memory cells are used as the source of entropy in the proposed PUF architecture. These on-demand memory cells can be distributed across the combinational logic of various intellectual property (IP) blocks in a system on chip (SoC) design. They can also be synthesized with a standard logic synthesis tool to meet the area/power/performance constraints of a design. By aggregating the power-up states from multiple such memory cells, we can create a PUF signature or digital fingerprint of varying size. We evaluate the MeL-PUFsignature quality with both circuit-level simulations as well as with measurements in FPGA devices. We show that MeL-PUFprovides high-quality signatures in terms of uniqueness, randomness, and robustness, without incurring large overheads. We also suggest additional optimizations that can be leveraged to improve the performance of MeL-PUF.

1 INTRODUCTION AND RELATED WORK

Physically unclonable functions (PUFs) have emerged as a popular mechanism for authentication. PUFs have been used as random number generators for crypto applications [15], as a countermeasure to defend against IP piracy [21], and to perform chip authentication [10].

The different PUF structures, proposed over the years, can be broadly classified into two classes based on the sources of randomness i) Delay PUFs and ii) Memory PUFs. Delay PUFs [4], exploit the variation in delay between two identical paths of a given design. Examples of delay PUFs include Ring Oscillator PUFs(ROPUF) [20], and Arbiter PUFs [11]. Memory PUFs on the other hand exploit the randomness introduced by the SRAM cells when powered on [12]. The PUF structures can also be classified into Strong vs Weak PUFs based on their ability to handle large input challenges [18]. PUFs will take a sequence of bits as input which controls the generation of a response. This combination is referred to as a challenge-response pair (CRP). Generally, strong PUFs refer to a PUF with multiple CRPs, meaning the number of CRPs increases exponentially as PUF size increase [5]. Therefore they can provide a larger range of responses with minimal overhead. A weak PUF will only output one response, meaning PUF size correlates to response size linearly [5].

Table 1: Table listing the properties of various PUFs

	[9]	[13]	[8]	[7]	[22]	[3]	MeL-PUF
Uniqueness	✓	✓	✓	✓	✓	✓	✓
Randomness	✗	✗	✗	✗	✓	✗	✓
Unclonability	✗	✗	✗	✗	✗	✗	✗
Reliability	✓	✓	✓	✓	✓	✓	✓
Robustness	✓	✓	✓	✗	✓	✓	✓
Synthesizability	✗	✗	✗	✗	✗	✗	✓
Resistance to Model building attacks	✗	✗	✗	✓	✗	✗	✓
Fully digital	✓	✓	✓	✓	✓	✓	✓

While strong PUF may appear to be the more suitable candidate the ability to input challenges and readout responses makes them vulnerable to model-building attacks [6]. Weak PUFs have shown resistance to model-building attacks making them more desirable for commercial applications [19]. Delay PUFs like Arbiter PUFs, and ROPUFs are examples of Strong PUFs, while Memory PUFs are examples of Weak PUFs.

An interesting observation here is that a majority of the PUF structures require dedicated structures leading to increased area and performance overheads. This makes them especially unsuitable for resource-constrained environments such as the Internet of Things applications. Strong PUFs are vulnerable towards model-building attacks while weak PUFs require specialized structures for implementation. Additionally, these structures are vulnerable to tampering attacks where the attacker could remove the PUF structure and thus bypass the authentication mechanism. Table 1 summarizes the capabilities of the existing PUFs reported in the literature.

In this paper, we present MeL-PUF, a novel fully synthesizable PUF structure obtained by integrating memory elements into the digital logic of a combinational circuit. Figure 1(a) illustrates the MeL-PUFstructure. MeL-PUFconsists of two cross-coupled inverters connected to form a bistable memory cell. Upon powering on, the values at the two inverter inputs are randomly initialized due to which they enter a meta-stable state. The value at the output stabilizes to either a 1 or a 0 at random. MeL-PUFconsists of a control logic comprising of a multiplexer and control signal. The control signal can be used to read the value of the bi-stable element. Figure 1(b) shows the proposed MeL-PUFstructure integrated into a digital design. To the best of our knowledge MeL-PUFis the first fully synthesizable PUF structure. We show that our proposed MeL-PUFstructure incurs low overhead, and can be incorporated into a wide variety of designs. We demonstrate the utility of MeL-PUFusing both simulation and hardware implementation.

The paper is organized as follows: we describe the MeL-PUFstructure in section 2. We discuss the evaluation of our proposed PUF structure along with its overheads in section 3. We highlight the utility of MeL-PUFin section 4.

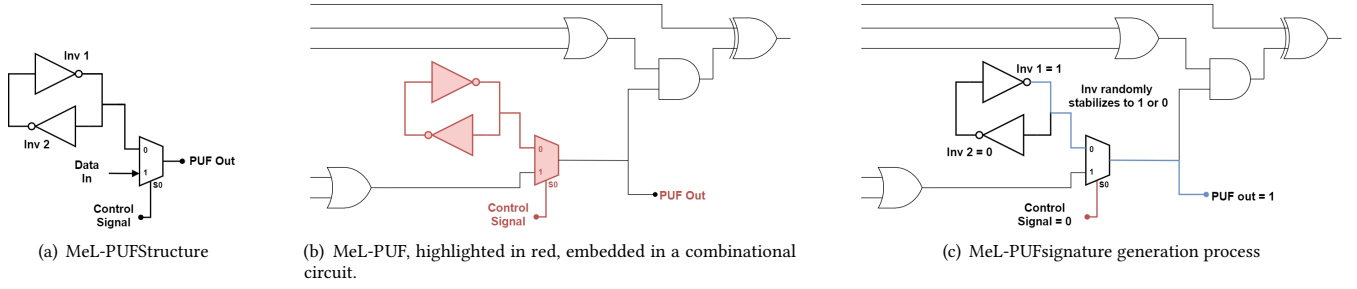


Figure 1: The logical structure, implementation, and working principle of MeL-PUF. Each element of MeL-PUF can be configured into a memory cell (cross-coupled inverter) using a control signal. The power-up states of the memory cells act as the entropy source for the PUF.

2 MEL-PUF: MEMORY IN LOGIC PUF

2.1 MeL-PUF Structure

Figure 1(a) illustrates the proposed MeL-PUF structure. MeL-PUF consists of two cross-coupled inverter structures and a control element, thus constituting the structure of a memory element, such as an SRAM cell. Upon startup, the output of the bistable element is unknown and is random, which is then used as our PUF response. The structure of the PUF allows us to distribute and place the PUF in the data-path of a combinational circuit as shown in Figure ?? . This is accomplished through the control MUX. A two-input MUX allows us to switch between the PUF response and logic data.

Figure 1(b) depicts MeL-PUF implementation where we incorporate bi-stable memory element in a circuit to create a PUF. The additional MeL-PUF circuitry is highlighted in red, with original paths in black. During power-up, the output of the memory cell results in an unknown state, which we use as our source of entropy. The output of one inverter is connected to a MUX which acts as the control element. When the control signal is low, the MUX allows the PUF signature to be captured at startup. When the control signal is high, then the circuit functions normally.

2.2 MeL-PUF Signature Generation

The data-paths for generating a response from the PUF are outlined in figure 1(c). The PUF structure can be inserted and distributed throughout a circuit as shown in figure 1(b). On startup, the bistable element enters a metastable state, similar to an SRAM cell. As such the state in which the bistable element stabilizes is unknown and random. In the example shown in figure 1(c), the value of inverter 1 stabilizes to 1 and is sampled by the control element. This is shown as the blue data-path. When the control signal, highlighted in red, is low the output of inverter 1 is sampled as the PUF output. Sampling multiple PUF elements and combining their response allows you to create a signature unique to the device or chip.

2.3 MeL-PUF Integration

In our proposed approach, we incorporate the PUF elements into the datapath or control logic of a combinational design. We accomplish this as described in the following steps:

- (1) Judiciously selecting the gates where the feedback loop can be created and adding the feedback loop there such that we

create a cross-coupled inverter with special emphasis on making it symmetric.

- (2) Controlling the feedback loop by incorporating MUXes or other control logic in the feedback path and control signals.
- (3) By connecting the output of the cross-coupled inverter to the scan chain (or to primary outputs using muxes).

3 EXPERIMENTAL SETUP AND RESULTS

PUFs demonstrate the following four properties [14]: uniqueness, reliability, unclonability, and randomness. Uniqueness is the ability of the PUF to produce distinct signatures for different challenges. Reliability is defined as the ability to produce the same response for the same input challenge every time. Unclonability is the property of a PUF that withstands against any replication, and randomness means that the corresponding PUF can generate random signatures for a wide variety of input challenges. We evaluate our proposed PUF structure based on these metrics using both transistor-level simulations and implementation on an FPGA.

3.1 MeL-PUF Simulation and Analysis

We create a transistor-level model of the MeL-PUF circuit in HSPICE using the 45 nm high-performance CMOS process node from Predictive Technology Model (PTM) [1]. We use an input clock frequency of 100 MHz signal to this circuit along with the nominal supply voltage, $V_{DD} = 1.0$ V. We initialize all the circuit nodes as '0' at the beginning of the simulation. We consider the manufacturing process variations by combining the effects of physical specifications such as t_{ox} , W , L , etc. into a single parameter- the threshold voltage, V_{th} [16]. We model these process variations as variations of V_{th} by using a Gaussian distribution for 10000 MeL-PUF circuit models/instances with $\sigma_{inter-die} = 25\%$. We apply the in-built parameter distribution function of HSPICE, AGAUSS, to shift/skew the transistor threshold values to generate this distribution as depicted in Fig. 2(a). To characterize the effect of manufacturing process variations, we perform Monte-Carlo simulation on power-up values at nominal temperature, $T_{NOM} = 25^\circ\text{C}$ on the generated model. Each Monte-Carlo simulation run results in a 1-bit power-up value for that specific MeL-PUF circuit instance, and we use that as a corresponding binary signature. Fig. 2(b) illustrates the gray colormap of collected power-up values for 10000 MeL-PUF instances,

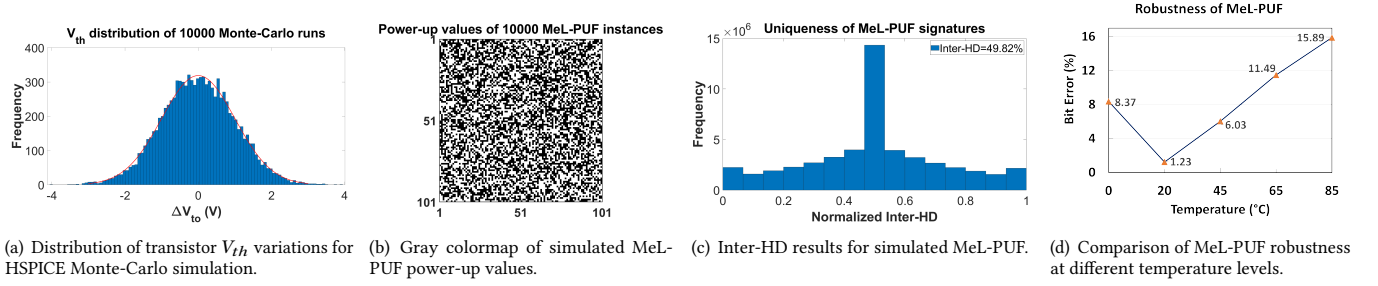


Figure 2: MeL-PUF evaluation using HSPICE simulation results over collected 64000 CRPs.

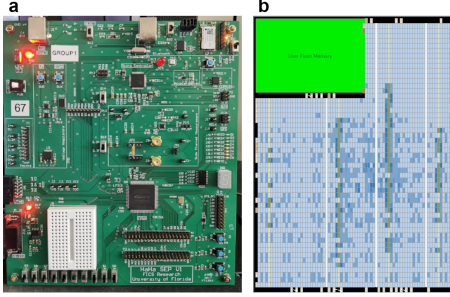


Figure 3: (a) Board used for PUF implementation. (b) image of Quartus Chip planner for the implemented circuit.

where the dark dots indicate power-up states of ‘1’ and white dots represent the ‘0’s. In our experiment, we discover that 5033 out of the total 10000 simulated circuit instances startup with ‘1’ and the rest appear to have a bias towards ‘0’ as their power-up values. To investigate the performance as a PUF, we build a circuit model with 64 instances of MeL-PUF for each Monte-Carlo simulation to collect 64-bit PUF responses from each run; thus, we collect 640000 power-up values/signatures from all 10000 runs. We evaluate the security performance of the simulated MeL-PUF in terms of uniqueness, robustness, and randomness.

3.1.1 Uniqueness Analysis. We assess the uniqueness of MeL-PUF by calculating the inter-chip Hamming distance (inter-HD). Inter-HD is the difference in number of bits obtained by applying the same signature to two different boards. Inter-HD is calculated using the formula described in equation 1.

$$\frac{2}{R(R-1)} \sum_{u=1}^{M-1} \sum_{v=u+1}^M \frac{HD(S_u, S_v)}{n} \times 100 \quad (1)$$

Fig. 2(c) illustrates the uniqueness results of the collected signatures (at $T_{NOM} = 25^\circ\text{C}$) in terms of inter-HD. Here, the X-axis shows the percentage of difference of bits between the responses, and the Y-axis shows the number of times the bit difference occurs. We observe that the simulation design of MeL-PUF demonstrates 49.82% inter-HD, which is very close to an ideal case.

3.1.2 Robustness Analysis. We use the intra-Hamming distance (intra-HD) for evaluating the robustness of MeL-PUF.

$$\frac{1}{x} \sum_{u=1}^x \frac{HD(S_u, S_v)}{n} \times 100 \quad (2)$$

intra-HD is the difference in response offered when two different challenges are applied to the same PUF implementation. intra-HD is estimated using equation 2. We assess the intra-HD by simulating the operation of MeL-PUF over five different temperature levels: 0, 20, 45, 65, and 85°C (at nominal $V_{DD} = 1.0\text{ V}$). Fig. 2(d) shows the percentage bit-errors in terms of average intra-HD at different temperature levels. We observed that the PUF exhibits 8.37%, 1.23%, 6.03%, 11.49%, and 15.89% bit-errors 0, 20, 45, 65, and 85°C respectively.

3.1.3 Randomness Analysis. To evaluate the randomness, we perform simulation on our MeL-PUF model and collect one million response bits to facilitate in assessing some tests in the NIST (National Institute of Standards and Technology) randomness test suite [2]. We observed that generated sequences successfully pass all of the performed tests at a p -value higher than 0.001. Thus we conclude that the simulated MeL-PUF responses are random with a confidence level of 99.9%.

3.2 Hardware-level Evaluation of MeL-PUF

We also validate our MeL-PUF structure by implementing it on an FPGA platform. We used a Max 10 FPGA (10M50SAE144C8G) based platform [17]. Figure 3(a) presents the layout of the FPGA board. We used ISCAS85 benchmark circuits to insert the MeL-PUF structure while ensuring that the LUTs were not simplified or combined with any other logic. Internal observation points are also added to the circuit observing the output of the control MUXes. These points are routed to RAM (Random Access Memory) and used to extract the signature through the in-system memory content editor of Quartus software. To test different regions of the board, LUT placements for the PUF are set using the assignment editor.

To evaluate the signatures generated by our design, we insert a set of PUFs into an ISCAS85 benchmark circuit for signature generation. This design is programmed to a Max 10 FPGA and we sample 1024-bit signatures from the circuit for ten boards. For each board, we sample five different LUT regions and collect four signatures per-region. These regions were used to calculate the uniqueness, reliability, and randomness of our PUF. Signatures are collected under nominal conditions (3.3 V at 25°C). Additionally, we also sampled the signatures under a range of voltages between 3 V - 1.97 V to quantify the robustness of our designed PUF.

3.2.1 Uniqueness. Figure 4(a) shows the histogram plotting the uniqueness between all boards. The X-axis shows the percentage of

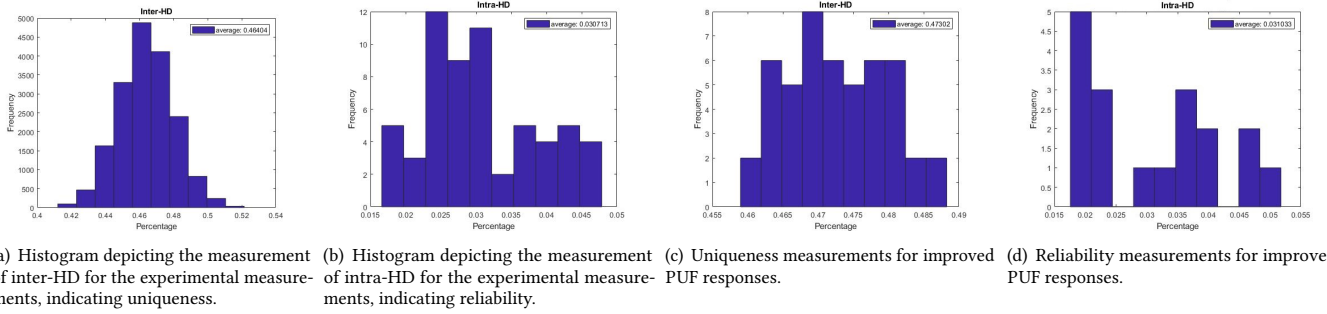


Figure 4: Figure showing the evaluation of MeL-PUFon FPGA. (a) represents the uniqueness, (b) shows the reliability results, (c) and (d) show the improvement in uniqueness and reliability using the optimizations described in section 4

different bits between signatures. The y-axis shows the frequency at which these differences occurred. The average inter-hamming distance is recorded for our results is 46.40%, giving us close to the ideal result of 50%.

3.2.2 Reliability. The reliability of MeL-PUF is calculated by comparing signatures from the same LUT region over multiple measurements. Certain LUTs may exhibit different levels of stability due to manufacturing variations. Figure 4(b) shows a histogram of reliability, giving our solution an average inter hamming distance is 3.07%.

3.2.3 Randomness. The Randomness evaluation of the experimental results is shown in table 2. We obtained the signatures from ten different boards and used these signatures for evaluating the randomness of MeL-PUF. We used the NIST Test Suite for our evaluation and performed the following tests on each signature sequence.

3.2.4 Robustness. As a measure of PUF robustness, voltage variations are also taken into account. In this case, the typical voltage supplied to the board is 3.3 V. We collect data for voltages between 3 V - 1.97 V and compare the signature to those of 3.3 V. The average Hamming distances are shown in the table 3. The average inter-HD between voltages is recorded as 7% and the intra-HD as 2%. Significant changes only begin occurring at 2.2 V when the inter-HD rose to 4%, with the highest being 13% at 1.97 V, the lowest the board could function. Above 2.2V, the variations were around 2.5% which is a reasonable variation. We observe that the reliability of the PUF is not significantly affected at different voltages.

4 ANALYSIS

4.0.1 Improvements to Uniqueness and Reliability. Since the routing of the LUTs is not perfect, there exists an asymmetry among the paths between the two LUTs. This results in a bias in the generated signatures. We observed that LUT towards the bottom of a LAB tended to have a higher delay. We leverage this to improve the uniqueness and reliability of the PUF signature. We chose 4 different PUF configurations D1-D4, as shown in Figure 5. We sample the signatures obtained from multiple regions of the board and eliminate the LUTs exhibiting bias. Figure 4(c) and Figure 4(d) show the improvement in inter-HD and intra-HD. We observed that inter-HD

rose to 47.30% while intra-HD reduced to 1.75% for configuration D4 shown in Figure 5(d).

4.0.2 PUF Distribution and Randomness. We also considered the effect of the adjacent LABs on the randomness of the PUF responses. We evaluated this by varying the PUF configuration as shown in Figure 5. We observed that the distribution that had the least number of overlaps resulted in the highest randomness values. We evaluated the four PUF configurations using the NIST test suite and present the results in table 2. Configuration D4 shown in Figure 5(d) resulted in the highest randomness values.

5 CONCLUSION

The emergence of the internet of things (IoT) era has necessitated low-cost, robust, and highly secure hardware-based authentication primitives. We have presented a novel PUF implementation paradigm that can be integrated into combinational logic and is distributed, synthesizable, easily configurable, and lightweight (in terms of area, power, performance overhead). Such a PUF implementation can serve as an attractive authentication primitive in diverse applications, including IoT. While the proposed PUF is a weak PUF and provides one-bit entropy per cell, it is capable of generating a high-quality signature in terms of uniqueness, randomness, and robustness. The PUF signatures can be easily read out through the scan chain. We have evaluated MeL-PUF implementations using simulation and FPGA platform with promising results. Our future work will include further optimization of the PUF design, analysis of the effectiveness of MeL-PUF further through measurements, and evaluation on large scale designs.

6 ACKNOWLEDGEMENT

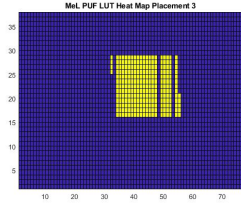
The work is funded in part by Defense Advanced Research Project Agency (DARPA) as part of the Automatic Implementation of Secure Silicon (AISS) program in collaboration with Northrop Grumman Corporation (NGC).

REFERENCES

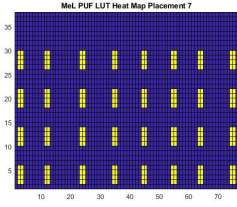
- [1] 2009. *Predictive Technology Model*. <http://ptm.asu.edu/>
- [2] 2010. *SP 800-22 Rev. 1a. A Statistical Test Suite for Random and Pseudorandom Number Generators for Cryptographic Applications*. Gaithersburg, MD, United States. <https://nvlpubs.nist.gov/nistpubs/Legacy/SP/nistspecialpublication800-22r1a.pdf>

Table 2: NIST Test Suite Results for MeLPUF signatures. Signatures from ten different boards (i.e., 10 different chips) are measured for each region. The results indicate the number of signatures are above the threshold for the passing p-value (0.001) and the uniformity of the p-value. Cumulative sums test is run on two different subsets of the signature, indicated by S_1 and S_2 .

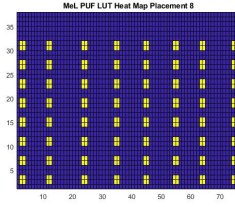
Test	D1		D2		D3		D4	
	No.of Passing Inputs	P-value	No.of Passing Inputs	P-value	No.of Passing Inputs	P-value	No.of Passing Inputs	P-value
Frequency	8/10	0.00000	7/10	0.00000	7/10	0.00000	10/10	0.53415
Block Frequency	10/10	0.35049	10/10	0.00204	10/10	0.00020	10/10	0.53415
Cumulative Sums S_1	8/10	0.00000	7/10	0.00000	8/10	0.00000	10/10	0.53415
Cumulative Sums S_2	6/10	0.00000	7/10	0.00000	8/10	0.00000	10/10	0.35049
Runs	8/10	0.00000	6/10	0.00000	6/10	0.00000	5/10	0.00000
Longest Run	9/10	0.01791	9/10	0.00888	10/10	0.21331	10/10	0.53415
Rank	10/10	0.00000	10/10	0.00004	10/10	0.00095	10/10	0.00095
FFT	10/10	0.00888	10/10	0.01791	10/10	0.06688	9/10	0.00888



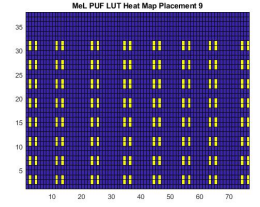
(a) D1: FPGA floor-plan showing the implementation of a clustered PUF.



(b) D2: FPGA floor-plan showing the implementation of a PUF implemented as 32×32 -bit clusters.



(c) D3: FPGA floor-plan showing the implementation of a PUF implemented as 64×16 -bit clusters with adjacent LABs.



(d) D4: FPGA floor-plan showing the implementation of a PUF implemented as 64×16 -bit clusters with no adjacent LABs.

Figure 5: FPGA floor-plans with both clustered and distributed MelPUF layouts. We performed experimental measurements with four different levels of spatial distribution of the PUF elements to analyze the effect of PUF cell placements.

Table 3: Average hamming distance between chip instances for a range of voltages.

Voltage	3.0V	2.65V	2.5V	2.2V	2.0V	1.96V
Inter-HD	2.6%	2.5%	2.3%	4%	12%	13%
Intra-HD	2.6%	2.4%	2.4%	2%	1.8%	1.8%

- [3] X. Wang A. R. Krishna, S. Narasimhan and S. Bhunia. 2011. MECCA: arobust low-overhead PUF using embedded memory array. In *CHES*. 407–420.
- [4] M. van Dijk B. Gassend, D. Clarke and S. Devadas. 2002. Silicon physical random functions. In *Proceedings of the 9th ACM conference on Computer and communications security*. New York, NY, USA, 148–160.
- [5] A. Babaei and G. Schiele. 2019. Physical Unclonable Functions in the Internet of Things: State of the Art and Open Challenges. *Sensors (Basel)* 19, 14 (July 2019).
- [6] L. Santiago et al. 2017. Realizing strong PUF from weak PUF via neural computing. In *IEEE International Symposium on Defect and Fault Tolerance in VLSI and Nanotechnology Systems (DFT)*. 1–6.
- [7] W. Liu et al. 2019. XOR-Based Low-Cost Reconfigurable PUFs for IoT Security. *ACM Trans. Embed. Comput. Syst.* 18, 3 (June 2019), 1–21.
- [8] A. Dawoud M. Niamat F. Amsaad, A. Sherif and S. Kose. 2018. A Novel FPGA-based LFSR PUF Design for IoT and Smart Applications. In *NAECON 2018 - IEEE National Aerospace and Electronics Conference*.
- [9] J. Zhou J. Gan and N. Wang. 2018. A FPGA-based RO PUF with LUT-Based Self-Compare Structure and Adaptive Counter Time Period Tuning. In *2018 IEEE International Symposium on Circuits and Systems (ISCAS)*. 1–5.
- [10] T. M. Bauer J. R. Hamlet and L. G. Pierson. 2014. Deterrence of Device Counterfeiting, Cloning, and Subversion by Substitution Using Hardware Fingerprinting.
- [11] B. Gassend G. E. Suh M. van Dijk J. W. Lee, Daihyun Lim and S. Devadas. 2004. A technique to build a secret key in integrated circuits for identification and authentication applications. In *2004 Symposium on VLSI Circuits. Digest of Technical Papers*. 176–179.
- [12] J. Jang and S. Ghosh. 2015. Design and analysis of novel SRAM PUFs with embedded latch for robustness. In *Sixteenth International Symposium on Quality Electronic Design*. 298–302.
- [13] Mengyang Li G. Qu Jiadong Wang, A. Cui and H. Li. 2016. An ultra-low overhead LUT-based PUF for FPGA. In *2016 IEEE Asian Hardware-Oriented Security and Trust (AsianHOST)*. 1–6.
- [14] R. Maes and I. Verbauwhede. 2010. Physically Unclonable Functions: A Study on the State of the Art and Future Research Directions. *Towards Hardware-Intrinsic Security* (2010), 3–37.
- [15] Charles W O'donnell, G Edward Suh, and Srinivas Devadas. 2004. PUF-based random number generation. In *MIT CSAIL CSG Technical Memo* 481 (2004).
- [16] H. Mahmoodi S. Mukhopadhyay and K. Roy. 2005. Modeling of failure probability and statistical design of SRAM array for yield enhancement in nanoscaled CMOS. 24, 12 (Dec. 2005), 1859–1880.
- [17] J. Vosatka S. Yang and S. Bhunia. 2017. Hardware Hacking Security Education Platform (HaHa SEP v2): Enabling Hands-On Applied Research of Hardware Security Theory & Principles. In *HOST*.
- [18] Z. M. Wang U. Roedig T. McGrath, I. E. Bagci and R. J. Young. 2019. A PUF taxonomy. *Applied Physics Reviews* 6, 1 (Feb. 2019).
- [19] J. S ölter G. Dror S. Devadas U. R ührmair, F. Sehnke and J. ürgen Schmidhuber. 2010. Modeling attacks on physical unclonable functions. In *Proceedings of the 17th ACM conference on Computer and communications security - CCS '10*. Chicago, Illinois, USA, 237.
- [20] C. Wang Y. Cui W. Liu, Y. Yu and M. O'Neill. 2015. RO PUF design in FPGAs with new comparison strategies. In *2015 IEEE International Symposium on Circuits and Systems (ISCAS)*. 77–80.
- [21] F. Koushanfar Y. Alkabani and M. Potkonjak. 2007. Remote Activation of ICs for Piracy Prevention and Digital Right Management. In *Proceedings of the 2007 IEEE/ACM international conference on Computer-aided design*. San Jose, California, USA, 674–677.
- [22] A. R. Krishna Yu Zheng and S. Bhunia. 2013. ScanPUF: Robust ultralow-overhead PUF using scan chain,. In *2013 18th Asia and South Pacific Design Automation Conference (ASP-DAC)*. 626–631.